

Helmholtz free energy of an anharmonic crystal to $O(\lambda^4)$. IV. Thermodynamic properties of Kr and Xe for the Lennard-Jones, Morse, and Rydberg potentials

R. C. Shukla and F. Shanes

Department of Physics, Brock University, St. Catharines, Ontario, Canada L2S 3A1

(Received 19 December 1984)

We have carried out a complete calculation of the various thermodynamic properties of Kr and Xe from the (λ^4) anharmonic perturbation theory proposed by Shukla and Cowley [Phys. Rev. B 3, 4055 (1971)], where λ is the Van Hove ordering parameter. To illustrate the effect of different potential functions on the various calculated thermodynamic properties, we have employed a nearest-neighbor central force model with the Lennard-Jones (LJ), Morse, and Rydberg interaction potentials. Along with the λ^4 results, we also present the results for the quasiharmonic (QH) and the λ^2 perturbation theory for all three potentials for each of Kr and Xe rare-gas solids. The LJ QH results are qualitative for most of the thermodynamic properties of Kr and Xe and best QH results are obtained with the Rydberg potential. The λ^2 perturbation theory results are poor beyond $\frac{1}{3}T_m$ (T_m is the melting temperature) for the LJ potential and somewhat better for the Morse and Rydberg potentials. Best results for β (volume expansivity) and C_p (specific heat at constant pressure) are obtained with the λ^4 theory and the Morse potential. The convergence of the perturbation expansion improves with the addition of λ^4 contributions and the expansion remains valid up to 40% of T_m for the LJ potential. The range of expansion is much higher for the other two potentials. Whereas the curvature of most of the calculated curves for the various thermodynamic properties for the λ^2 theory is incorrect, the corresponding curves from the λ^4 theory have the correct curvature. The cancellation among the λ^2 and λ^4 contributions is most dramatic for the LJ potential and less so for the other two potentials. As T approaches T_m , only the Rydberg-potential results, for the λ^2 theory, appear to be sensible compared with the other two potentials for most of thermodynamic properties of Kr and Xe.

I. INTRODUCTION

There are several theories of anharmonicity from which the equation of state of a solid can be calculated. Among these theories, extensive numerical results have been reported for the rare-gas solids from the various self-consistent phonon theories of anharmonicity such as the first-order self-consistent theory¹ (SC1), the improved self-consistent theory² (ISC), and the lowest-order perturbation theory³ (PT). In the lowest-order PT calculation, a nearest-neighbor (NN) Lennard-Jones (LJ) 6-12 interaction potential was employed by Klein, Horton, and Feldman.³ The same potential was also used in the SC1 and ISC calculations by Goldman *et al.*² Klein *et al.*³ concluded that the lowest-order PT breaks down beyond $\frac{1}{3}T_m$ where T_m is the melting temperature. One might expect that the results for the various thermodynamic properties will improve if the next set of perturbation contributions is added to the lowest-order PT in the calculation of the equation of state of a rare-gas solid. The contributions just mentioned consist of the evaluation of eight contributions to the Helmholtz function (F). The formal expressions for the eight contributions have been derived by Shukla and Cowley.⁴ Numerical results for the nearest-neighbor 6-12 LJ potential were obtained by Shukla and Cowley⁴ and Shukla and Wilk⁵ at one volume $V=V_0$, the 0-K equilibrium volume. They also assessed the convergence of the PT expansion but did not calculate the equation of state.

However, in a recent publication Shukla and Cowley⁶ have calculated the equation of state for a NN model of a LJ solid and compared the thermodynamic results for the λ^2, λ^4 theories and the Monte Carlo method for the same model potential. As expected the λ^4 PT did produce an improvement in the calculated thermodynamic properties but only up to about 40% of T_m .

The objective of this paper is to calculate the equation of state of Kr and Xe by including the above-mentioned corrections to the lowest-order PT. This means that we calculate for Kr and Xe the lattice constant, volume expansion, adiabatic and isothermal bulk moduli, specific heat at constant pressure (C_p) and constant volume (C_v), and Grüneisen parameter (γ), from the quasiharmonic theory (QH); from the lowest-order (λ^2) PT, where λ is the Van Hove perturbation expansion parameter; and finally from the corrections added to the λ^2 PT, i.e., the perturbation theory of $O(\lambda^4)$.

The two basic ingredients in calculations of this type are (i) phonon frequencies (ω) and (ii) the derivatives of a potential function $\phi(r)$. In the above calculations we have employed a two-parameter Lennard-Jones potential, and one each of three-parameter Morse and Rydberg potentials, to bring out the effect of potential functions in such calculations. As stated earlier, the λ^2 PT breaks down beyond $\frac{1}{3}T_m$ but this conclusion arrived at by Klein *et al.*³ was valid for the LJ potential; whether it remains true for other potential functions is not known. Our calculation will shed some light on this question.

In Sec. II we summarize briefly the calculation of the λ^4 contributions to F . The details are omitted because the calculation procedure has been given previously by Shukla and Wilk.⁵ In the previous calculations the LJ-potential parameters were determined by including the harmonic zero-point energy contributions derived by Domb and Salter.⁷ In the present work we do not use the Domb-Salter approximation of zero-point energy in the determination of the potential parameters. The determination of the potential parameters for the three potential functions and the calculation of the equation of state are presented in Sec. III. The numerical results and discussion are presented in Sec. IV and finally the conclusions of this work are given in Sec. V.

To summarize, then, two central questions are addressed in this paper. (1) How are the results for the various thermodynamic properties affected when different potential functions are used in the calculations to a given order of perturbation theory? (2) How are the results for the various thermodynamic properties affected when, for a given potential function, the order of the perturbation theory is changed from λ^2 to λ^4 ?

These questions are answered by calculating the various thermodynamic properties for Kr and Xe to $O(\lambda^2)$ and $O(\lambda^4)$ PT for two-parameter LJ and three-parameter Morse and Rydberg potentials. The convergence of the perturbation expansion is much better with the latter two potentials as compared with the LJ potential and the λ^2 and λ^4 results are very much *dependent* on the choice of a potential function. The results for the Morse and Rydberg potentials are different from LJ not because of one extra parameter but due to their different functional forms. For the various thermodynamic properties the λ^2 PT gives the wrong curvature for all three potential functions, and this is corrected when the λ^4 contributions are added.

There are some systematics apparent with respect to the choice of potential or the order of the perturbation theory. For all three potentials there are similarities in the QH and λ^2 results and a varying degree of corrections from the λ^4 PT to most of the physical properties for both elements Kr and Xe. Only for LJ is the situation extreme where the addition of the λ^4 contribution brings the λ^2 results back towards the QH values. Similar behavior is seen in the results for Morse and Rydberg but to a much lesser degree. A large anharmonic contribution to C_p is found for the LJ potential but not for the other two.

Since the results⁶ for the LJ potential are not transferable to other potentials, this is the first serious attempt to compare the thermodynamic results of the different orders of PT (λ^2 and λ^4), calculated exactly, for a crystal model from different potential functions. The existing literature does not tell us how the equation of state looks for the Morse and Rydberg potentials even for the lowest-order λ^2 PT, let alone the $O(\lambda^4)$ PT.

II. HELMHOLTZ FREE ENERGY (F) to $O(\lambda^4)$

Shukla and Cowley⁴ have derived *all* the contributions to F of $O(\lambda^4)$ for a centrosymmetric crystal. Since in this paper we are dealing with such a crystal we need to evaluate the *eight* contributions (diagrams) given by Eqs. (9)–(28) in Shukla and Cowley.⁴ On expanding the finite-temperature expressions for these eight contributions to F , we find their high-temperature limit ($T > \Theta_D$; Θ_D is the Debye temperature) expressions. In this paper we will identify the various contributions to F from the diagrams given in Fig. 2 of Shukla and Cowley⁴ by a subscript. Thus F_{2a} represents the contribution of diagram 2a (Fig. 2 of Ref. 4), etc., and the high-temperature limit expansion gives the following expressions for $F_{2a}, F_{2b}, \dots, F_{2h}$: To $O(T^3)$ and $O(T)$,

$$F_{2a} = \frac{\hbar^3}{48N^2} \sum_{1,2,3} \frac{\Phi_{1\bar{1}2\bar{2}3\bar{3}}}{\omega_1^2 \omega_2^2 \omega_3^2} \left[\left(\frac{k_B T}{\hbar} \right)^3 + \frac{\omega_1^2}{4} \left(\frac{k_B T}{\hbar} \right) \right], \quad (1)$$

$$F_{2b} = \frac{-\hbar^3}{16N^2} \sum_{1,2,3,4} \frac{\Phi_{1\bar{1}2\bar{2}3\bar{3}4\bar{4}}}{\omega_1^2 \omega_2^2 \omega_3^2 \omega_4^2} \left[\left(\frac{k_B T}{\hbar} \right)^3 + \frac{\omega_1^2}{6} \left(\frac{k_B T}{\hbar} \right) \right], \quad (2)$$

$$F_{2c} = \frac{-\hbar^3}{12N^2} \sum_{1,2,3,4} \frac{\Phi_{123\bar{1}\bar{2}\bar{3}\bar{4}\bar{4}}}{\omega_1^2 \omega_2^2 \omega_3^2 \omega_4^2} \left[\left(\frac{k_B T}{\hbar} \right)^3 + \frac{\omega_4^2}{12} \left(\frac{k_B T}{\hbar} \right) \right], \quad (3)$$

$$F_{2d} = \frac{\hbar^3}{8N^2} \sum_{1,2,3,4,5} \frac{\Phi_{134\bar{5}\bar{5}\bar{1}\bar{2}\bar{3}\bar{4}}}{\omega_1^2 \omega_2^2 \omega_3^2 \omega_4^2 \omega_5^2} \left[\left(\frac{k_B T}{\hbar} \right)^3 + \frac{\omega_5^2}{12} \left(\frac{k_B T}{\hbar} \right) \right], \quad (4)$$

$$F_{2e} = \frac{-(k_B T)^3}{48N^2} \sum_{1,2,3,4} \frac{|\Phi_{1234}|^2}{\omega_1^2 \omega_2^2 \omega_3^2 \omega_4^2}, \quad (5)$$

$$F_{2f} = \frac{-(k_B T)^3}{16N^2} \sum_{1,2,3,4,5,6} \frac{\Phi_{134\bar{1}\bar{5}\bar{6}\bar{2}\bar{3}\bar{4}\bar{5}\bar{6}}}{\omega_1^2 \omega_2^2 \omega_3^2 \omega_4^2 \omega_5^2 \omega_6^2}, \quad (6)$$

$$F_{2g} = \frac{(k_B T)^3}{8N^2} \sum_{1,2,3,4,5} \frac{\Phi_{124\bar{5}\bar{1}\bar{2}\bar{3}\bar{4}\bar{5}}}{\omega_1^2 \omega_2^2 \omega_3^2 \omega_4^2 \omega_5^2}, \quad (7)$$

$$F_{2h} = \frac{-(k_B T)^3}{24N^2} \sum_{\substack{1,2,3, \\ 4,5,6}} \frac{\Phi_{123}\Phi_{145}\Phi_{2\bar{5}6}\Phi_{3\bar{4}6}}{\omega_1^2\omega_2^2\omega_3^2\omega_4^2\omega_5^2\omega_6^2}, \quad (8)$$

$$\begin{aligned} \Phi_{123\dots n} &= \Phi(\mathbf{q}_1, j_1; \mathbf{q}_2, j_2; \dots; \mathbf{q}_n, j_n) \\ &= \Delta(\mathbf{q}_1 + \mathbf{q}_2 + \dots + \mathbf{q}_n) \Phi \left[\frac{1}{2M^{n/2}} \right] \sum'_l \sum_{\alpha_1, \alpha_2, \dots, \alpha_n} \phi_{\alpha_1 \alpha_2 \dots \alpha_n}(|\mathbf{r}_l|) \\ &\quad \times e_{\alpha_1}(\mathbf{q}_1, j_1) e_{\alpha_2}(\mathbf{q}_2, j_2) \dots e_{\alpha_n}(\mathbf{q}_n, j_n) \prod_{k=1}^n \left[1 - e^{i\mathbf{q}_k \cdot \mathbf{r}_l} \right], \end{aligned} \quad (9)$$

where in Eqs. (1)–(8), N represents the number of unit cells, \hbar is the Planck's constant divided by 2π , k_B is the Boltzmann constant, and T is the temperature. The numerals 1–6 appearing under summation signs and as subscripts in Φ functions and ω 's represent collectively the wave vectors \mathbf{q}_i and branch indices j_i , where $i=1, 2, \dots, 6$. The bars over the subscripts denote the negative wave vector. Thus the phonon frequency $\omega_i = \omega(\mathbf{q}_i, j_i)$. In Eq. (9), M is the atomic mass, \mathbf{r}_l is a vector of the direct lattice, $e_{\alpha}(\mathbf{q}, j)$ is the α th component of the eigenvector, and $\phi_{\alpha_1 \alpha_2 \dots \alpha_n}(|\mathbf{r}_l|)$ is the Cartesian derivative of a two-body potential $\phi(r)$, where each of the indices $\alpha_1, \alpha_2, \dots, \alpha_n$ assume the Cartesian values x, y , and z . The prime over the l summation in Eq. (9) indicates the omission of the origin point, and finally the Δ function in Eq. (9) is unity if the argument is zero or a vector of the reciprocal lattice, and zero otherwise.

There is little need to reproduce here the free energy expressions of $O(\lambda^2)$ because all the contributions to this order have been evaluated before by Shukla and MacDonald.⁸ We have retained terms of $O(T)$ in Eqs. (1)–(8) because, as we will see in the next section, they make small contributions to the quantities involving the first derivative of T .

Substituting Eq. (9) into Eqs. (1)–(8), all the eight contributions of $O(T^3)$ and four contributions of $O(T)$ arising in F_{2a} , F_{2b} , F_{2c} , and F_{2d} have been evaluated for a range of volumes by the method presented in Shukla and Wilk.⁵ All the necessary Brillouin-zone (BZ) sums, arising in the plane-wave method and the evaluation of closed loops in F_{2a} , F_{2b} , F_{2c} , and F_{2d} (Fig. 2 of Ref. 4), were evaluated with step length $Z=30$ (which gives 108 000 points in the whole BZ). The plane-wave method was used in the calculation of F_{2e} and the scanning method in the calculation of F_{2f} , F_{2g} , and F_{2h} . We have used 500 wave vectors in the calculation of F_{2f} and a combination of 215 odd and even wave vectors in the calculation of F_{2g} and F_{2h} . The normalization procedure remains the same as in Shukla and Wilk.⁵

III. DETERMINATION OF THE POTENTIAL PARAMETERS AND CALCULATION OF THE EQUATION OF STATE

As mentioned in the Introduction, we have calculated the lattice constant (a); volume expansion (β); adiabatic and isothermal bulk moduli (B_S and B_T , respectively); C_p ,

C_v , and γ from the QH; and λ^2 and λ^4 equations of state from three different potential functions. The two-parameter LJ and the three-parameter Morse and Rydberg potentials are given by

$$\Phi_{LJ}(r) = \epsilon \left[\left(\frac{r_0}{r} \right)^{12} - 2 \left(\frac{r_0}{r} \right)^6 \right], \quad (10)$$

$$\Phi_M(r) = \epsilon (e^{-2\alpha(r-r_0)} - 2e^{-\alpha(r-r_0)}), \quad (11)$$

$$\Phi_R(r) = -\epsilon [1 + \alpha(r-r_0)] e^{-\alpha(r-r_0)}, \quad (12)$$

where subscripts distinguish the three potentials and the parameters ϵ and r_0 denote well depth and the nearest-neighbor distance, respectively. The parameter α appearing in Eqs. (11) and (12) represents the steepness of the potential function.

We determine ϵ and r_0 of Φ_{LJ} from the experimental values⁹ of the sublimation energy (L) and the lattice constant (a_0) at 0 K. The three parameters of Φ_M or Φ_R are determined from L, a_0 and the experimental value¹⁰ of the 0-K bulk modulus (B_T^0). The necessary equations for determining the parameters are

$$F = (U + E_h)_{r=r_0} = -L, \quad (13)$$

$$P = - \left[\frac{\partial F}{\partial V} \right]_{V=V_0} = 0, \quad (14)$$

$$B_T^0 = V_0 \left[\frac{\partial^2 F}{\partial V^2} \right]_{V=V_0}, \quad (15)$$

where, in Eqs. (13) and (14), U is the static energy, V_0 is the volume at 0 K, P denotes the pressure, and the harmonic zero-point energy E_h is defined by

$$\begin{aligned} E_h &= \frac{1}{2} \hbar \sum_{\mathbf{q}, j} \omega(\mathbf{q}, j) = \frac{1}{2} \hbar \left[\frac{2B}{M} \right]^{1/2} \sum_{\mathbf{q}, j} \lambda(\mathbf{q}, j) \\ &= \frac{1}{2} \hbar \left[\frac{2B}{M} \right]^{1/2} h(a_1), \end{aligned} \quad (16)$$

where $\lambda(\mathbf{q}, j)$ is the dimensionless frequency which is evaluated for a range of volumes [characterized by a parameter a_1 involving the first and second derivatives of $\Phi(r)$] from the elements of the dynamical matrix. Once again the details of this type of calculation can be obtained from Shukla¹¹ and Ref. 8. The quantity B in Eq.

(16) is defined by $[\Phi^{11} - (1/r)\Phi^1]_{r=r_0}$ and the function $h(a_1)$ is evaluated by performing the BZ sum for $Z=30$. The calculated values of $h(a_1)$ in the range $-0.02 \leq a_1 \leq 0.10$ are presented in Table I. For computational purposes they were fitted to an exponential sixth-degree polynomial as in Shukla and MacDonald.⁸ The potential parameters for the LJ, Morse, and Rydberg potential functions were determined from the data presented in Table II. The parameters are presented in Table III.

Once the parameters of the potential function are determined, the calculation of the various thermodynamic properties from the QH and λ^2 and λ^4 equations of state is carried out, from the following expressions:

$$E_{\text{QH}} = U + F_{h_1} + F_{h_2}, \quad (17)$$

$$E_{\lambda^2} = E_{\text{QH}} + F_{\lambda^2}, \quad (18)$$

$$E_{\lambda^4} = E_{\lambda^2} + F_{\lambda^4}, \quad (19)$$

where $U = 6N\phi(r_0)$ and F_{h_1}, F_{h_2} are the high-temperature (HT) limit expressions for the quasiharmonic Helmholtz free energy derived by Shukla and MacDonald [Eqs. (3)–(4a) in Ref. 8]. The HT limit expression for F_{λ^2} is also given in Ref. 8. The calculation of the HT limit expressions for F_{λ^4} of $O(T^3)$ and $O(T)$ has been presented in Sec. II of this paper. The final expressions are too lengthy to reproduce here but they can be obtained from Shukla and Wilk.⁵

The minimization of Eqs. (17)–(19) at a given T yields the minimum volume $V(T)$. The Newton-Raphson (NR) method was used to find $V(T)$, and the first and second derivatives of E , needed in the NR method, were obtained analytically. The other thermodynamic properties were calculated from the following equations:

$$C_v = -T \left[\frac{\partial^2 F}{\partial T^2} \right]_V, \quad (20)$$

$$B_T = V \left[\frac{\partial^2 F}{\partial V^2} \right]_T, \quad (21)$$

$$\beta = -\frac{1}{B_T} \left[\frac{\partial^2 F}{\partial V \partial T} \right], \quad (22)$$

$$C_p = C_v + TVB_T\beta^2, \quad (23)$$

$$B_s = (C_p/C_v)B_T, \quad (24)$$

$$\gamma = \frac{\beta VB_T}{C_v}. \quad (25)$$

TABLE I. Dimensionless sum $h(a_1)$ as a function of a_1 .

a_1	$h(a_1)$
0.10	4.706 165
0.08	4.590 436
0.06	4.471 387
0.04	4.348 685
0.02	4.221 932
0.00	4.090 646
-0.02	3.954 230

TABLE II. Data for fitting the interatomic potential. Nearest-neighbor distance r_0 at 0 K (Ref. 9), sublimation energy L (Ref. 9), bulk modulus B_T^0 at 0 K (Ref. 10).

Element	r_0 (Å)	L (10^{11} erg/mole)	B_T^0 (kbar)
Kr	3.992	1.115	34.5
Xe	4.336	1.602	36.0

IV. RESULTS AND DISCUSSION

The results for the various thermodynamic properties of Kr and Xe calculated from the QH and λ^2 and λ^4 equations of state along with their experimental values¹⁰ are presented in Figs. 1–7 and 8–14, respectively. To bring out the effect of employing the different potential functions on the various thermodynamic properties, we have calculated them for the nearest-neighbor interaction LJ, Morse, and Rydberg potentials. The curves for the various equation-of-state calculations presented in Figs. 1–7 and 8–14 are labeled with subscripts LJ, M , and R for each of the three potential functions, respectively. Now, to simplify the discussion of these results, we will discuss them separately in the order of LJ, Morse, and Rydberg.

A. LJ results for Kr and Xe

It is interesting to note that for both Kr and Xe, the QH results are too high for a_T , β , C_v , C_p , and γ and too low for B_T and B_s , as compared to the experimental values.

The results can at best be described as qualitative. The λ^2 results, which are obtained by the addition of the λ^2 terms to the QH free energy, are in agreement with experiment only at the lowest temperatures (slightly higher than Θ_D). Beyond this temperature the λ^2 curves for *all* thermodynamic properties (except a_T and bulk moduli) start bending downwards as T approaches T_m . In general, our λ^2 results are essentially the same as those calculated by Klein, Horton, and Feldman.³

The addition of the λ^4 terms to the $(\text{QH} + \lambda^2)$ free energy improves the agreement with experiment only slightly again in the neighborhood of Θ_D . In contrast to the λ^2 curves with downward curvature, now the λ^4 curves have an upward curvature. The λ^4 curve for a_T runs parallel, but below, the QH curve. For C_v , the λ^4 curve rises above the QH curve. Compared to the experimental values the λ^2 and λ^4 results diverge in opposite directions, the former

TABLE III. Potential parameters for NN interaction LJ, Morse, and Rydberg potentials. r_0 (Å), α (Å⁻¹), ϵ (10^{-14} erg).

	LJ	Morse	Rydberg
Kr	$\epsilon=3.248$	$\epsilon=3.254$	$\epsilon=3.254$
	$r_0=3.965$	$r_0=3.969$	$r_0=3.971$
		$\alpha=1.556$	$\alpha=2.194$
Xe	$\epsilon=4.577$	$\epsilon=4.576$	$\epsilon=4.576$
	$r_0=4.318$	$r_0=4.321$	$r_0=4.322$
		$\alpha=1.375$	$\alpha=1.941$

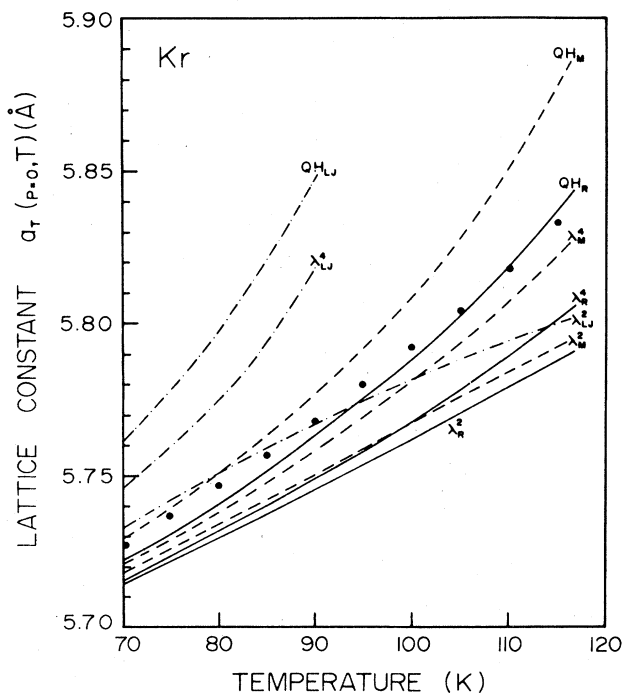


FIG. 1. Lattice constant (a_T) at zero pressure for Kr. Points, experimental data; dot-dashed lines, NN LJ potential; dashed lines, NN Morse potential; solid lines, NN Rydberg potential. QH with subscripts LJ, M, and R denote quasi-harmonic results; similarly, λ^2 and λ^4 denote perturbation-theory results to $O(\lambda^2)$ and $O(\lambda^4)$, respectively.

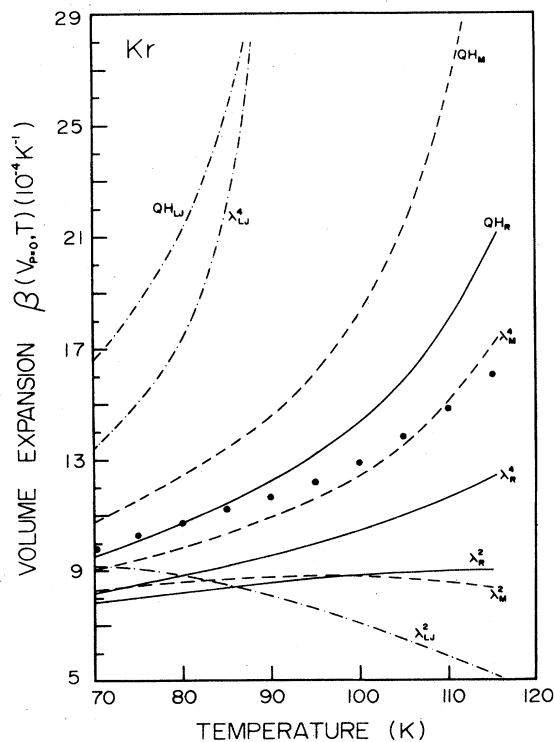


FIG. 2. Volume expansion (β) for Kr. Points and lines have the same meaning as in Fig. 1.

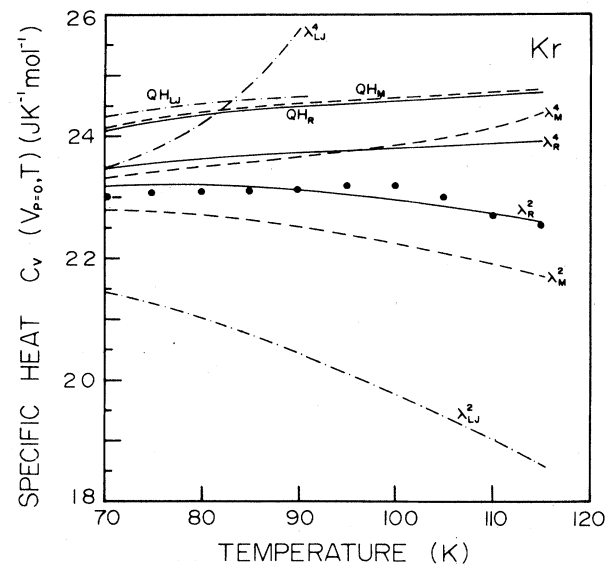


FIG. 3. Specific heat at constant volume (C_v) for Kr. Points and lines have the same meaning as in Fig. 1.

being lower and the latter being higher. It seems that there is some degree of cancellation between the λ^2 and λ^4 terms of the PT to the contribution of the various thermodynamic properties. Only for Xe can a considerable degree of agreement be seen between the λ^4 results and the experimental values for C_v , C_p , B_T , and B_S in the temperature range 60–100 K.

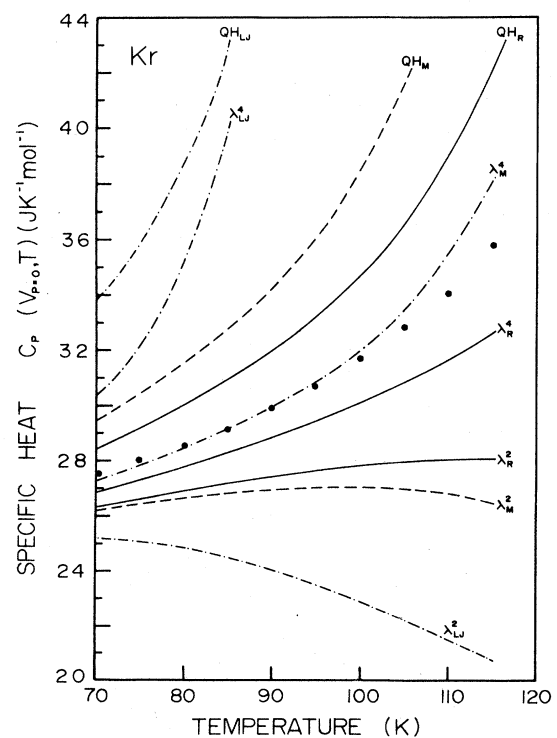


FIG. 4. Specific heat at constant pressure (C_p) for Kr. Points and lines have the same meaning as in Fig. 1.

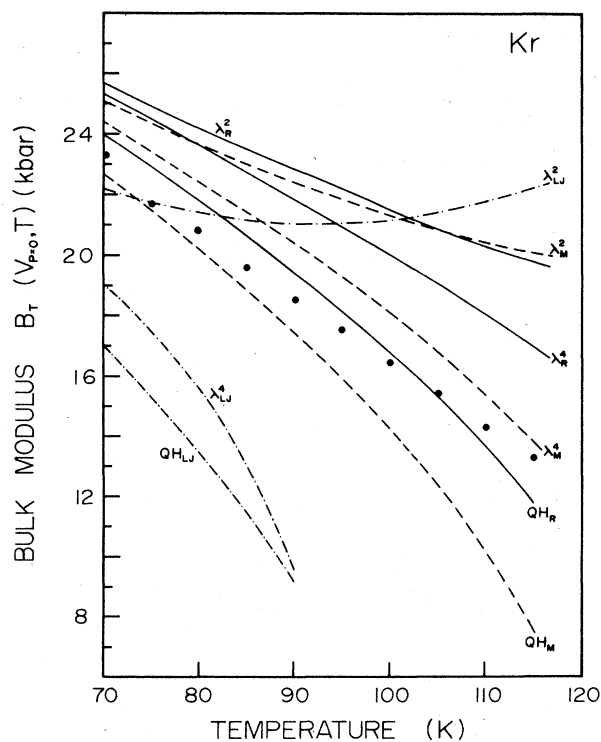


FIG. 5. Isothermal bulk modulus (B_T) for Kr. Points and lines have the same meaning as in Fig. 1.

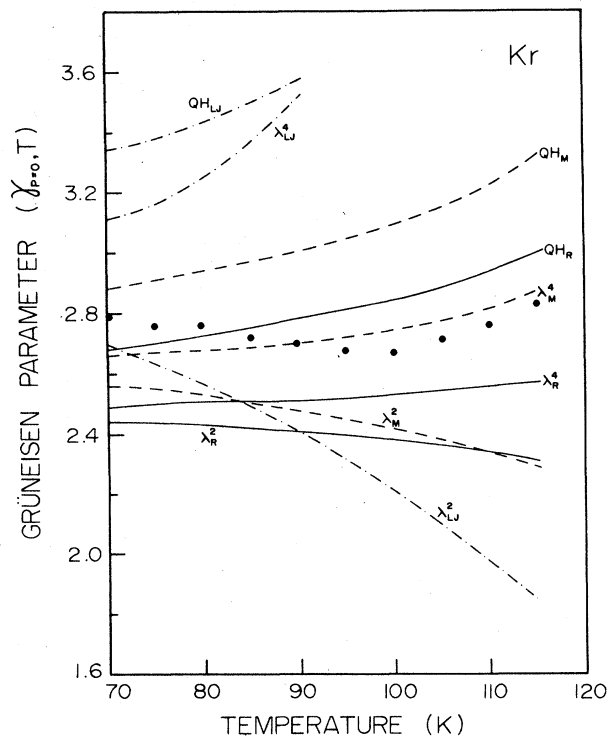


FIG. 7. Grüneisen parameter (γ) for Kr. Points and lines have the same meaning as in Fig. 1.

B. Morse results for Kr and Xe

In general, for most of the thermodynamic properties of Kr and Xe the QH results for the Morse potential are much closer to the experimental values than those of the LJ potential. The QH curves for B_T and B_s are very close to the experimental points. Now the λ^2 curves are not as

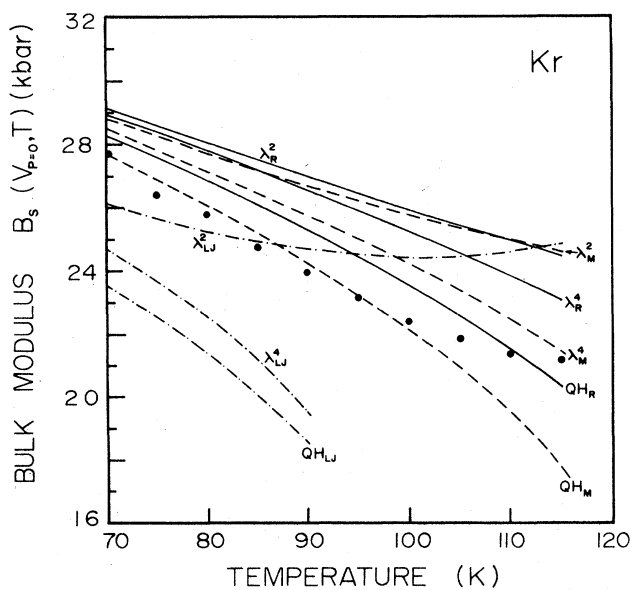


FIG. 6. Adiabatic bulk modulus (B_s) for Kr. Points and lines have the same meaning as in Fig. 1.

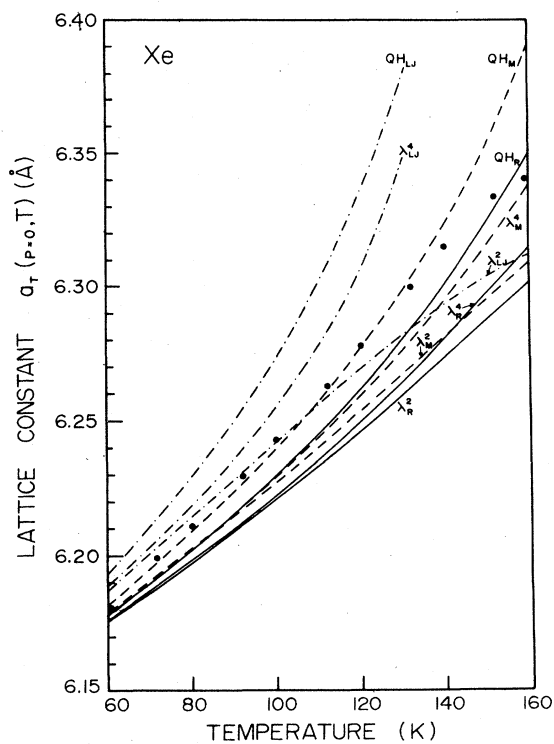


FIG. 8. Lattice constant (a_T) at zero pressure for Xe. Points and lines have the same meaning as in Fig. 1.

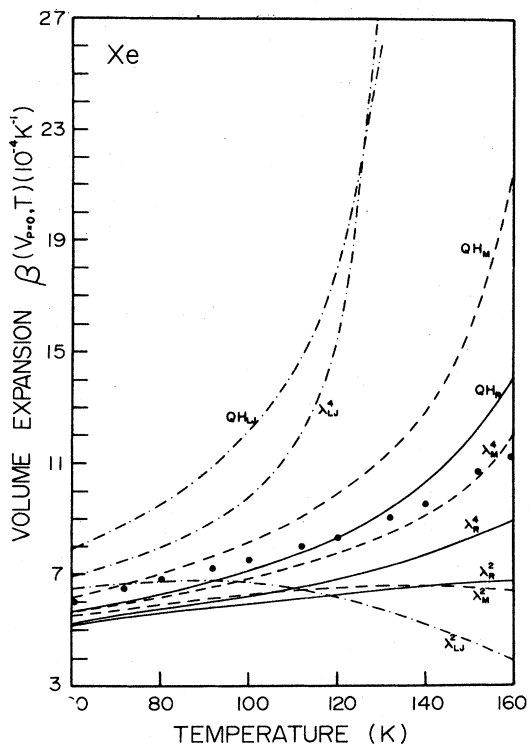


FIG. 9. Volume expansion (β) for Xe. Points and lines have the same meaning as in Fig. 1.

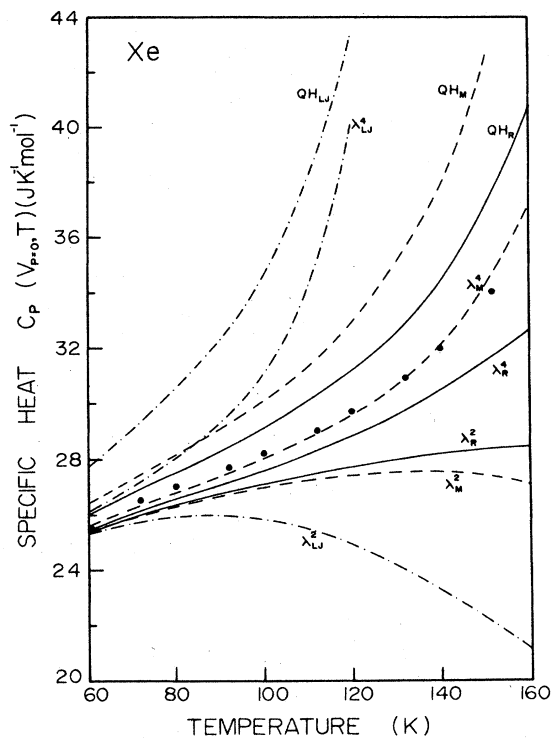


FIG. 11. Specific heat at constant pressure (C_P) for Xe. Points and lines have the same meaning as in Fig. 1.

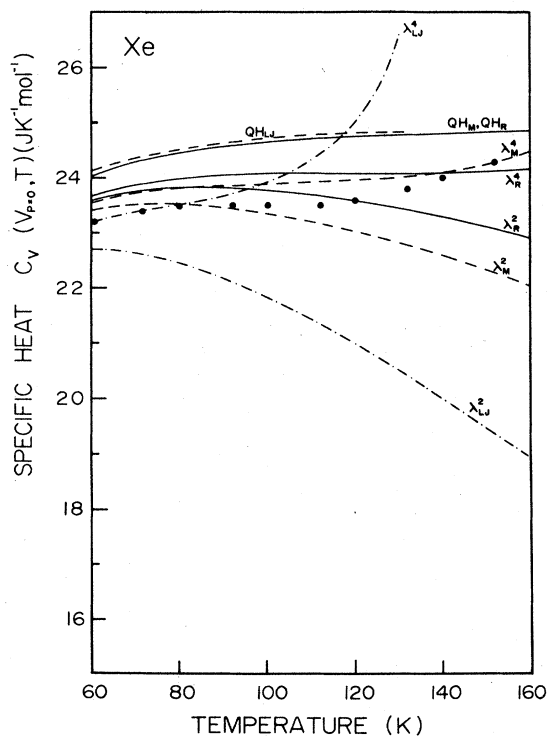


FIG. 10. Specific heat at constant volume (C_V) for Xe. Points and lines have the same meaning as in Fig. 1.

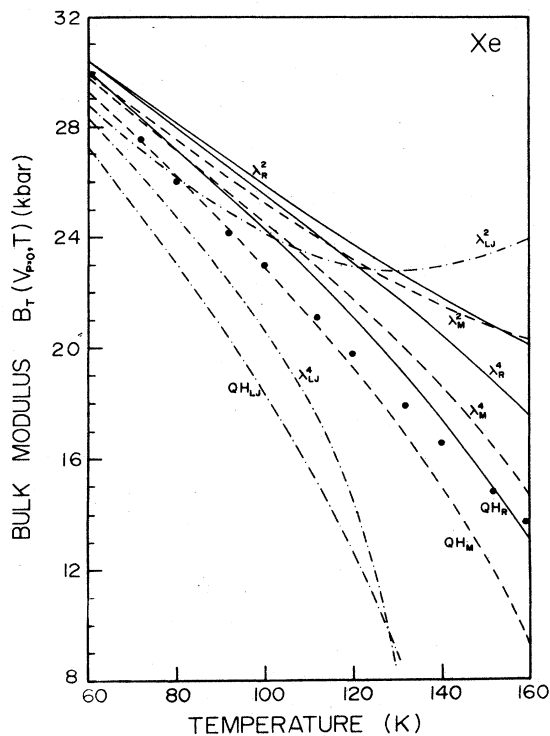


FIG. 12. Isothermal bulk modulus (B_T) for Xe. Points and lines have the same meaning as in Fig. 1.

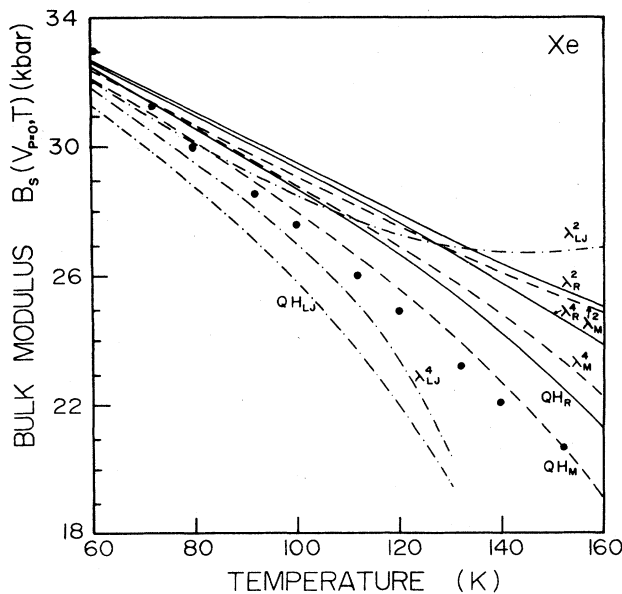


FIG. 13. Adiabatic bulk modulus (B_s) for Xe. Points and lines have the same meaning as in Fig. 1.

low as the corresponding curves of the LJ potential and the curves do not bend downward. Only a slight curvature can be seen in these curves in the region of $T \sim T_m$. For Kr the shape of the C_v curve is correctly given by the λ^2 equation-of-state calculation although the calculated curve lies lower than the experimental points.

The addition of the λ^4 terms produces a marked improvement in results for both Kr and Xe. For Kr the a_T , β , C_p , and γ results are very well reproduced by the λ^4 theory in the entire temperature range up to $T \sim T_m$, and a similar statement is true for Xe in the calculation of a_T , β , C_v , and C_p . The best agreement can be seen for C_p between the λ^4 results and the experimental values for both Kr and Xe.

C. Rydberg results for Kr and Xe

The best QH results are obtained from the Rydberg potential. For example, the QH results for a_T , β , C_p , B_T , and γ , for Kr, are closer to the experimental values than the QH results from the other two potentials, whereas C_v is just about the same as that obtained from the Morse potential. The same thing is true for Xe, except for γ . As in the case of the other two potentials, the addition of the λ^2 terms lowers the values of the thermodynamic properties and a further addition of the λ^4 terms raises them towards the QH results. Once again some degree of cancellation exists between the λ^2 and λ^4 contributions to the various thermodynamic properties of Kr and Xe. It seems that the best results for C_v , for Kr, are given by the λ^2 theory from the Rydberg potential.

The QH results for the three potentials for a property α , for Kr and Xe, are in the following order: $\alpha_{LJ} > \alpha_M > \alpha_R$ in the case of a_T , β , C_v , C_p , and γ with α_R being closer to the experimental value. For B_T and B_s , the above order is reversed. Most of the λ^2 curves, for all

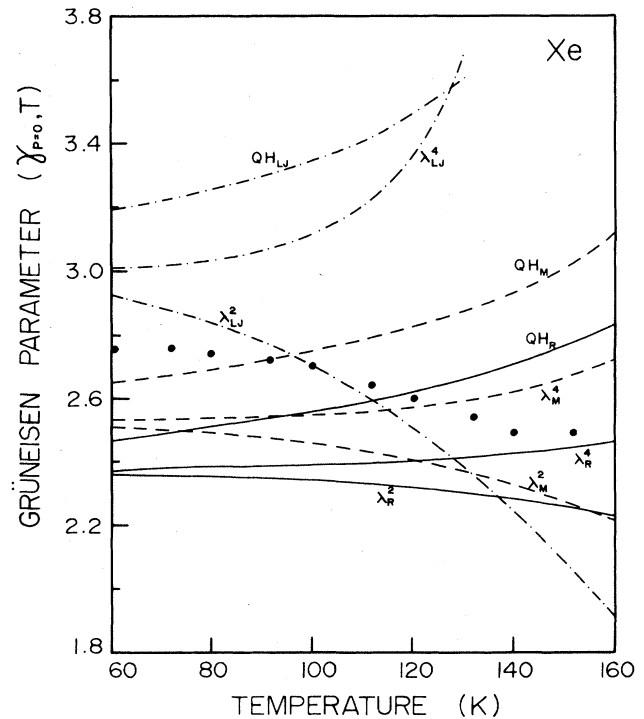


FIG. 14. Grüneisen parameter (γ) for Xe. Points and lines have the same meaning as in Fig. 1.

three potentials, have the wrong curvature, except for Kr, where the λ^2 C_v curve for the Rydberg potential passes right through the experimental points.

Although we have included terms of $O(T)$ in the equation-of-state calculations of $O(\lambda^4)$, i.e., Eq. (19), the effect of these terms was just about negligible. The potential parameters of the LJ potential obtained here without the Domb-Salter approximation of the zero-point energy are in good agreement with those given in Horton⁹ which were obtained by employing the Domb-Salter approximation.

V. CONCLUSIONS

We can draw several conclusions from the results of the above calculations. The results for the various thermodynamic properties definitely improve with the λ^4 theory. The improvement is marginal for the LJ potential. The range of validity of the perturbation expansion is extended from 25% of T_m for the λ^2 theory to about 40% of T_m for the λ^4 theory. The use of the other two potentials produces far better convergence for the λ^2 theory. Excellent results for the volume expansion (β) and specific heat (C_p) are obtained for the Morse potential with the λ^4 theory for both Kr and Xe. Even the QH results are quite reasonable with the Rydberg potential. Best results are obtained with the Rydberg potential for the λ^2 theory.

ACKNOWLEDGMENTS

One of us (R. C. S.) wishes to acknowledge the support of the Natural Sciences and Engineering Research Council of Canada.

- ¹P. F. Choquard, *The Anharmonic Crystal* (Benjamin, New York, 1967).
- ²V. V. Goldman, G. K. Horton, and M. L. Klein, *Phys. Rev. Lett.* **21**, 1527 (1968); M. L. Klein, V. V. Goldman, and G. K. Horton, *J. Phys. Chem. Solids* **31**, 2441 (1970).
- ³M. L. Klein, G. K. Horton, and J. L. Feldman, *Phys. Rev.* **184**, 968 (1969).
- ⁴R. C. Shukla and E. R. Cowley, *Phys. Rev. B* **3**, 4055 (1971).
- ⁵R. C. Shukla and L. Wilk, *Phys. Rev. B* **10**, 3660 (1974).
- ⁶R. C. Shukla and E. R. Cowley, *Phys. Rev. B* **31**, 372 (1985).
- ⁷C. Domb and L. S. Salter, *Philos. Mag.* **43**, 1083 (1952).
- ⁸R. C. Shukla and R. A. MacDonald, *High Temp. High Pressures* **12**, 291 (1980).
- ⁹G. K. Horton, *Am. J. Phys.* **36**, 93 (1968).
- ¹⁰P. Korpiun and E. Lüscher, in *Rare Gas Solids*, edited by M. L. Klein and J. A. Venables (Academic, New York, 1976), Vol. II.
- ¹¹R. C. Shukla, *Int. J. Thermophys.* **1**, 73 (1980).